ARTICLE

Evaluation of Phonon-level Density of UO_2 by Molecular Dynamics Simulation

Hui-fen Zhang[a], Gan Li[b], Xiao-feng Tian[a], Tao Gao[a]*

a. Institute of Atomic and Molecular Physics, Sichuan University, Chengdu 610065, China
b. National Key Laboratory for Physics and Chemistry, Mianyang 621907, China

(Dated: Received on April 18, 2011; Accepted on June 15, 2011)

Molecular dynamics calculation of UO_2 in a wide temperature range are presented and discussed. The calculated lattice parameters, mean square displacements, and dynamic property of phonon-level density of the velocity auto-correlation functions for UO_2 are provided. The Morelon potential and the Basak potential are employed. It confirms that the calculated lattice parameters using the Basak potential are in nearly perfect agreement with the reported values. The models successfully predict mean square displacement and Bredig transition. Furthermore, the phonon-level density of uranium dioxide are discussed. The intensity of phonon-level density increases with temperature, and the properties of UO_2 are characterized by large thermal vibrations rather than extensive disorder.

Key words: Molecular dynamics, Phonon-level density, Velocity auto-correlation function, Uranium dioxide

I. INTRODUCTION

Uranium-based materials attract much interest owing to their technological and environmental implication as well as for theoretical prospects. Uranium dioxide (UO_2) is an important material for nuclear industry. It is the usual fuel used for pressurized heavy water reactors, in the energy sources, which have played the most important role so far and will do in the future. Especially, the properties of UO_2 at high temperature are of great interest for the safety development and management of the nuclear reactor system, hence, the physicochemical properties and the nuclear characteristics of fuel materials need to be understood deeply.

As for the theoretical calculations, on the electronic scale there is still a challenge for the structure simulations owning to the localization effect of the f electrons coming from the strong electron-electron interaction. However, recent advances in computer power and simulation technique have allowed us to simulate the uranium-based materials behavior on the atomic scale. Since the pioneering works by Benson *et al.* [1] and Dolling *et al.* [2], two classes of inter-atomic potentials for UO_2 have been discussed. Many molecular dynamic (MD) studies of uranium dioxide have been performed to estimate a series of thermal properties [3−5]. A previous investigation of UO_2 using molecular dynamics simulation was reported by Walker and Catlow [6]. More recently, the molar specific heat and the thermal conductivity of UO_2 have been investigated by Yamada *et al.* [7], who developed a series of rigid-ion potentials for UO_2 using non-formal charges with fixed ionicity. Not long after, MD simulations have been performed to study the melting point using the inter-atomic potentials with the partially ionic model potential [8−12]. Experimentally, Infrared spectra of stoichiometric and hyperstoi-chiometric for uranium dioxide were measured by Allenet *et al.* [13]. Raman spectra were measured on the stoichiometric UO_2 [14−20], Manara and Renker measured the micro-Raman spectroscopy of stoichiometric and hyperstoi-chiometric for UO_2 [21]. These results are basic for the analysis of many stages of the nuclear fuel cycle. Unfortunately, to our knowledge, there is scarcely information on MD study of density of states (DOS) of the velocity auto-correlation functions for UO_2 available in the literature.

There are two principal factors to determine the reliability of the simulations. One is the number of ions taken in the ensemble, the other is the quality of the inter-atomic potentials used to represent the system. Inter-atomic potential functions are the essential part of the MD simulation. To some extent, all pair potentials developed for UO_2 are based on Catlows' original work [22]. In this work, we describe the density of states of power spectrum of the velocity autocorrelation functions for UO_2 using the rigid-ion potential developed by Morelon *et al.* [23] and Basak *et al.* potential [8], and predict whether the technique provides a promising way of studying the spectrum of nuclear fuel oxides.

*Author to whom correspondence should be addressed. E-mail: gaotao2010@gmail.com, Tel./FAX: +86-28-85405234

II. MOLECULAR DYNAMIC SIMULATION

A. Inter-atomic potential function

We applied two types of an inter-atomic potential function. The potential developed to data for UO_2 has been optimized by fitting the grid parameter, the elastic constants, the cohesive energy, *etc.* by Morelon *et al.* [23]. The U−U and U−O interaction potential appeared with the Born-Meyer-Huggins (BMH) analytic form to describe the non-Coulombic interactions:

$$U(r) = A\exp\left(-\frac{r}{B}\right) - \frac{C}{r^6} \tag{1}$$

where A, B, and C are the parameters of empirical potential for UO_2. The values of the inter-atomic potential function parameters are summarized in Table I. The BMH term of the U−U interaction is assumed to be zero since U−U distances are always large enough that the results are unaffected by the short-range BMH potential, and the $1/r^6$ term of the U−O interaction is neglected because the attraction is dominated by the electrostatic component [23]. As show in the Jackson *et al.* model [24], the potential for the O−O interaction is defined by intervals:

$$V_{\mathrm{OO}}(r) = \begin{cases} A_{\mathrm{OO}}\exp\left(-\dfrac{r}{B_{\mathrm{OO}}}\right), & r > 1.2\ \text{Å} \\ \text{Fifth degree polynomial}, & 1.2\ \text{Å} < r < 2.1\ \text{Å} \\ \text{Third degree polynomial}, & 2.1\ \text{Å} < r < 2.6\ \text{Å} \\ -\dfrac{C_{\mathrm{OO}}}{r^6}, & r < 2.6\ \text{Å} \end{cases} \tag{2}$$

Classical pair wise interaction that is essentially a BMH type potential model along with the Morse potential has been chosen. Such a combined potential model was originally used by Kawamura [25] for studying silicate and other oxide structures and subsequently by Yamada *et al.* [7] and later by Basak *et al.* [8] for UO_2.

$$U(r) = \frac{z_i z_j e^2}{r_{ij}} + f_0(b_i + b_j)\exp\left(\frac{a_i + a_j - r}{b_i + b_j}\right) - \frac{c_i c_j}{r_{ij}^6} + D_{ij}\{[\exp(-\beta_{ij}(r_{ij} - r_{ij}^*) - 1]^2 - 1\} \tag{3}$$

where z_i and z_j are the effective partial electronic charges on the ith and jth ions, r is the atom distance, r_{ij}^* is the bond length of the anion-cation pair in vacuum, a and b are the characteristic parameters depending on the ion species. In this potential function, D_{ij} and β_{ij} describe the depth and the shape, respectively. The first term is the Coulomb interactions while the second term denotes the core repulsion, and the third one accounts for van dar Wall's weak attraction. The last term which is called Morse-type [26] potential corresponds to the covalent contribution. The values of this inter-atomic potential function parameter are given in Table II.

TABLE I The parameters of empirical potential for UO_2 (uranium charge of +3.227252 and oxygen charge of −1.613626).

	U−U pair	U−O pair	O−O pair
A	0.0	566.498	Defined by polynomials
B	0.0	0.42056	Eq.(1)
C	0.0	0.0	

TABLE II The potential parameters of UO_2 (uranium charge of +2.4 and oxygen charge of −1.2).

	U−U pair	U−O pair	O−O pair
a/nm	0.326	0.354	0.382
b/pm	32.7022	32.7022	32.7022
c/(J nm^6)			3.81×10^{15}
β/nm^{-1}		0.165	
D/meV		577.45	
r^*/μm		22.39	
f_0/(eV/nm)	0.422		
ζ	0.6		

B. Simulation techniques

UO_2 holds stable fluorite structure (CaF_2 type), each unit cell contains four U^{4+} and eight O^{2+}. The MD calculation was performed for a system of 768 ions (cations: 256, anions: 512) that was constructed with an array of 4×4×4 super-cells in three mutually orthogonal directions.

In the present study, the MD simulations have been performed using DL-POLY program, a large-scale MD simulation package available from Daresbury laboratory [27]. The simulations were made in the temperature range 300−3000 K at zero pressure, the constant pressure-temperature (NPT) simulation was employed using Nose-Hoover thermostat to control the temperature. The Coulomb term has been calculated by an Ewald summation technique [28]. The atomic motion was obtained from the calculated forces via numerical integration, Verlet leapfrog algorithm [29], using a unit time step Δt of 2.0 fs with a real space cutoff of 0.1 nm. The periodic boundary conditions were considered. At the start of the calculation, the initial velocity of each atom was chosen to take a random velocity. At the desired temperature, the MD trajectories were generated with a total run of 10^5 time step, including 10^4 time step of equilibrium run.

III. RESULTS AND DISCUSSION

A. Lattice parameters

Some experimental data on lattice parameter together with the calculated lattice parameters, as a func-

DOI:10.1088/1674-0068/24/04/399-404

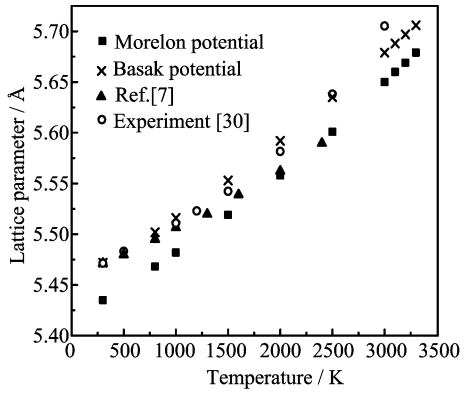

FIG. 1 Variation of lattice parameters of UO_2 with temperature from 300 K to 3500 K using Morelon potential and Basak potential.

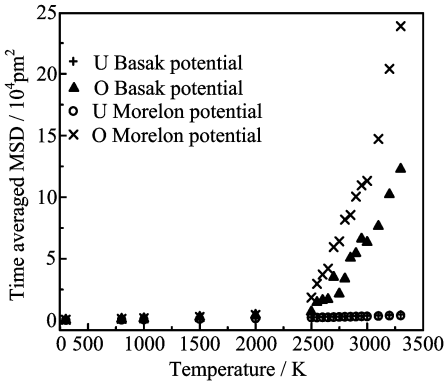

FIG. 2 Variation in time-averaged MSD of UO_2 with temperature from 300 K to 3500 K.

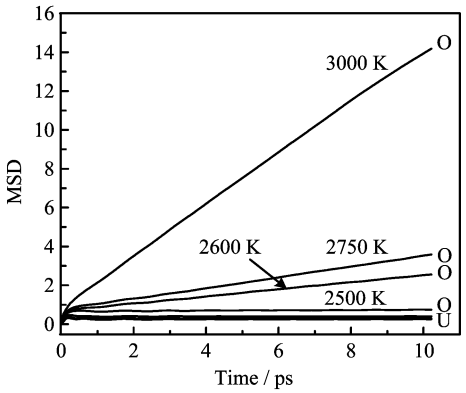

FIG. 3 The MSD of uranium and oxygen atoms in UO_2 as a function of time.

tion of temperature, are presented in Fig.1. Obviously, the calculated results with the Basak potential are in agreement with the experimental values by Martin [30], especially, up to 2500 K. At the higher temperature, the deviation which increases with temperature may result from the formation of Frenkel defects or the relatively large thermal expansion. However, the calculated values using the Morelon potential always underestimate the experimental data of lattice parameters by 0.96% in the range of temperature. The inadequacy of the potential model or the values of the potential parameters always results in the deviations, since the potential parameters used in present work are fitted at the low temperature, they may not be good for the estimation of the structure where the lattice expansion may be considerable.

B. Mean square displacement and Bredig transition

The mean square displacement (MSD) can be expressed as follows: [31]

$$\langle |r(t) - r(0)|^2 \rangle = \frac{1}{NN_t} \sum_{n=0}^{N} \sum_{t=t_0}^{N_t} |r_n(t+t_0) - r_n(t_0)|^2 (4)$$

where $r_n(t)$ is the position of nth particle at time t. N and N_t are total number of particle and total time step, respectively, t_0 is the initial time step. It is a measure of the average distance for the given atoms in a system. The slope of the MSD, considered for long time intervals, is related to the self-diffusion constant D that is straightforward to explain the anomalous increase of the diffusion rate coefficient at the transition. The so-called Bredig transition is connected with a disorder in the non-metal sub-lattice and with a dramatic rise of anion electrical conductivity [32], is characterized by a smooth peak in the heat capacity, it has been reported that a diffuse transition occurs at a value close to the ionic melt [33, 34].

We show the mean-square displacements at several temperatures in Fig.2, and Fig.3 provides the MSD of uranium and oxygen atoms in UO_2 as a function of time using Basak potential. It can be seen that there are very large and anisotropic thermal motions of the oxygen atoms from 2500 K to 3000 K, while U atoms have the low mobility. The Bredig transition of UO_2 was reported as 0.84 Tm at 2610 K [35] and 0.8 Tm as suggested by Browning *et al.* [36]. Our calculations show the existence of the Bredig transition is confirmed in the MD cell at 2500−3000 K (UO_2 melts at 3150 K). The diffusion coefficient of one of the constituent atom becomes comparable to that of liquids above the transition temperature. So the detailed study of the transition occurring in the crystal lattice at elevated temperatures is essential to understand the thermal properties. The transition temperature obtained with two potential models from the present calculations is in agreement with the experimental data. That is to say, from 2500 K to 3000 K oxygen diffusivity increases sharply, it is an indication of being the oxygen super-ionic conductor. It is a clear manifestation that simulated Bredig transition is not an inherent outcome of the potential model used; rather it is probably depends on the crystal structure

DOI:10.1088/1674-0068/24/04/399-404

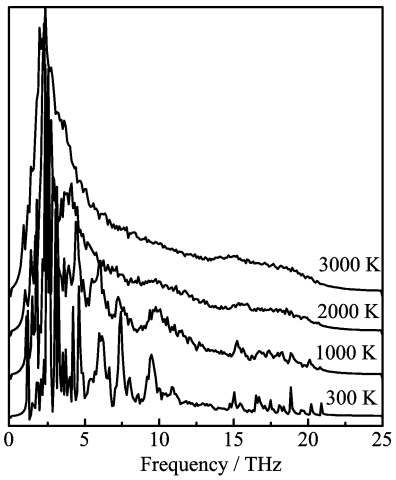

FIG. 4 Phonon-level density calculated by the velocity auto-correlation function for UO_2 in the NPT ensemble with temperature, using Morelon potential.

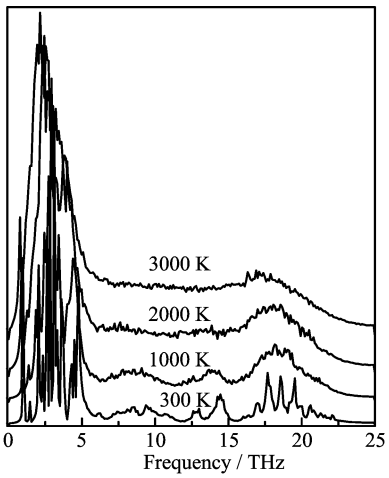

FIG. 5 Phonon-level density calculated by the velocity auto-correlation function with temperature by Basak potential.

and the ioncity of the material at high temperature.

C. Phonon-level density

Analysis of the velocity auto-correlation function (VACF) and the power spectra is a powerful tool for the elucidation of microscopic molecular motions. It gives a connection among the experimental, theoretical, and simulation works of the dynamic system. In this section, the phonon-level densities evaluated by VACF have been discussed. The VACF $C_{vv}(t)$ is defined as [37]:

$$c^i_{vv}(t) = \frac{\langle v^i(0)v^i(t)\rangle}{\langle v^i(0)v^i(0)\rangle} \tag{5}$$

$$\langle v^i(0)v^i(t)\rangle = \frac{1}{NN_0}\sum_{t_0=1}^{N_0}\sum_{j=1}^{N}[v^i_j(t+t_0)v^i_j(t_0)] \tag{6}$$

where i denotes x, y, and z directions, and t_0 is the origin time. $v^i_j(t)$ is the velocity of the center-of mass at time t. The summation in equation incorporates the number of atoms of a given atom type or the entire set of atoms for a total VACF.

The VACF can then be used to obtain the power spectrum of the velocity by the Fourier transform shown:

$$\rho(\omega) = \int_0^\infty \frac{\langle \vec{v}(t)\vec{v}(0)\rangle}{\langle \vec{v}(0)\vec{v}(0)\rangle}\exp(-i\omega t)\mathrm{d}t \tag{7}$$

the velocity power spectrum is very similar to the phonon spectrum and therefore this feature is calculated to investigate the vibrational properties of the materials. In other words, the phonon-level density can be obtained from the power spectrum of the VACF in MD simulation.

Figures 4 and 5 show the phonon-level density of vibrational spectra for UO_2 with several temperatures by Morelon potential and Basak potential, respectively. The calculated dispersion at the low temperature is in agreement with available curves from Refs. [10, 11] with two types of inter-atomic potential function, which are the BMH potential with the fully ionic model (FIM) and the BMH potential with the partially ionic model (PIM).

For the Morelon potential, the phonon-level density shows several peaks between 0−6 and 16−20 THz at 300 K, and the intensity of the low-frequency part is much lower than that of the high-frequency part. With increasing temperature, at 1000 K, the peaks of the low-frequency part die down, whereas, the total intensity slightly increases compared to 300 K; some relatively low peaks in the high-frequency part disappear, and, to some extent, the intensities increase. Up to 2000 K, the entire range has no high-frequency peak, only has two little peaks in the low frequency part, and the curve displays much smoother than that of 1000 K. There is only a vibrational peak at about 3 THz in the high-frequency part at 3000 K, and the intensity is the highest of all.

It undergoes similar transformation in the entire temperature range for the Basak potential. The oscillation frequency of peak is shifting to the low temperature part. And the whole intensities are progressively increasing, especially, for the higher frequency part. The peaks at the higher frequencies of this range are primarily due to vibrational motions of the crystal about its lattice sites. However, the result of Basak potential has an obvious change trends. In addition, the frequency ranges of the appearing peak are closer to the experimental data at 430, 450, 467, 575, 580, and 630 cm^{-1} [14, 15, 38, 39].

That can illustrate the results with Basak and Morelon potentials are available for evalution of vibrational properties. Maybe, some experimental values are

DOI:10.1088/1674-0068/24/04/399-404

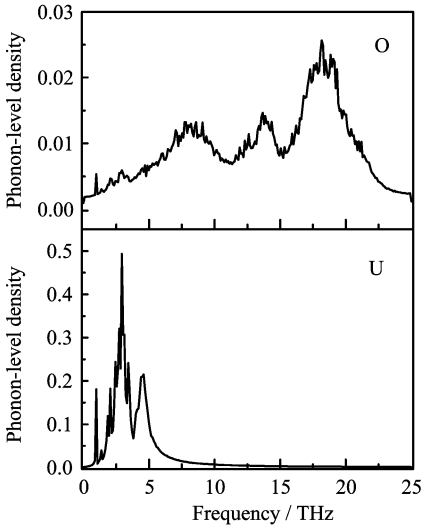

FIG. 6 Phonon-level density calculated by VACF for U ion and O ion at 1000 K with Basak potential.

not in agreement with our calculated data, since they should be attributed to electronic scattering rather than to a fluorite-like atom scale vibrational frequency.

Phonon-level density calculated by the velocity autocorrelation function for U and O atoms with the Basak potential at 1000 K is shown in Fig.6. The frequency spans the spectral range up to 25 THz, while uranium contribution is restricted up to 12 THz, and the oxygen contributes over the entire frequency range. It shows that uranium atoms have the low frequency component, while oxygen atoms have a high one which due to thermal motions in the system from their intensity.

It is consistent with results which elaborate the MSD of O atoms that begins to increase, while there is no significant change for that of U atoms. That is, oxygen atoms become more active and diffusive beyond 2500 K; the diffusion of uranium atoms is hardly visible, even at very high temperature. Uranium atoms have only a small vibration near their original locations owing to the defect in the high temperature or its large mass.

Oxygen sub-lattice of UO_2 is thermally less stable than its uranium sub-lattice, and, at sufficiently high temperature, becomes almost completely disordered with a large fraction of oxygen atoms occupying randomly regular or interstitial positions that lead to the formation of kinds of defects [40].

IV. CONCLUSION

MD simulations have been applied to evaluate the phonon-level density of power spectra of velocity autocorrelate functions for UO_2 using two types of interatomic potential function from 300 K to 3000 K. The lattice parameters were calculated from the Basak potential and in good agreement with existing experimental data. In the meanwhile, results for UO_2 showed both the mean square displacement and the existence of a Bredig transition. The transition results obtained by both potentials were in resemblance with the literature values.

Finally, the MD simulation showed the phonon-level density, which was evaluated by the velocity autocorrelation function in solid UO_2. The overall descriptions of the phonon-level density were presented by the two types of inter-atomic potential function. With the increasing temperature, the whole intensity is progressively increased, especially, for the higher frequency part. The properties of UO_2 are characterized by large thermal vibrations. Cations have the low frequency component, while oxygen has a high one. The results may be applicable to evaluate the spectrum of solid UO_2 in the future.

V. ACKNOWLEDGMENTS

We are very grateful for Hai-lan Zhou for helpful discussions and Dr. Shun-ping Shi and Tao Liu for practical help.

[1] G. C. Benson, P. I. Freeman, and E. Dempsey, J. Am. Ceram. Soc. **6**, 43 (1962).
[2] G. Dolling, R. A. Cowley, and A. D. Woods, Can. J. Phys. **43**, 1397 (1965).
[3] C. R. A. Catlow, Proc. R. Soc. A **353**, 533 (1977).
[4] P. J. D. Lindan and M. J. Gillan, J. Phys.: Condens. Mater. **3**, 3929 (1991).
[5] S. Higuchi, J. Nucl. Sci. Technol. **35**, 833 (1998).
[6] J. R. Walker and C. R. A. Catlow, J. Phys. C **14**, 979(1981).
[7] K. Yamada, K. Kurosaki, M. Uno, and S. Yamanaka, J. Alloys. Compd. **307**, 10 (2000).
[8] C. B. Basak, A. K. Sengupta, and H. S. Kamath, J. Alloys. Compd. **360**, 210 (2003).
[9] T. Arima, K. Idemitsu, Y. Inagaki, Y. Tsujita, M. Kinoshita, and E. Yakub, J. Nucl. Mater. **389**, 149 (2009).
[10] T. Arima, S. Yamasaki, Y. Inagaki, and K. Idemitsu, J. Alloys Compd. **400**, 43 (2005).
[11] T. Arima, S. Yamasaki, Y. Inagaki, and K. Idemitsu, J. Alloys Compd. **415**, 43 (2006).
[12] E. Yakub, C. Ronchi, and D. Staicu, J. Chem. Phys. **127**, 094508 (2007).
[13] G. C. Allen, J. A. Crofts, and A. J. Griths, J. Nucl. Mater. **62**, 273 (1976).
[14] G. Keramidas and W. B. White, J. Chem. Phys. **59**, 1561 (1973).
[15] P. R. Gravies, Appl. Spectroscopy **44**, 1665 (1990).
[16] P. G. Marlow, J. P. Russel, and J. R. Hardy, Philos. Mag. **14**, 409 (1966).
[17] G. C. Allen, I. S. Butler, and N. A. Tuan, J. Nucl. Mater. **144**, 17 (1987).
[18] J. Schoenes, J. Chem. Soc. Faraday Trans. 2 **83**, 1205 (1987).

DOI:10.1088/1674-0068/24/04/399-404

[19] S. Blumenroeder, H. Brenten, E. Zirngiebl, R. Mock, G. Guentherodt, J. D. Thompson, Z. Fisk, and J. Naegele, J. Magn. Magn. Mater. **76**&**77**, 331 (1988).
[20] M. L. Palacios and S. H. Taylor, Appl. Spectroscopy **54**, 1372 (2000).
[21] D. Manara and B. Renker, J. Nucl. Mater. **321**, 233 (2003).
[22] C. R. Catlow, Proc. R. Soc. London A **353**, 533 (1977).
[23] N. D. Morelon, D. Ghaleb, J. M. Delaye, and L. V. Brutzel, Philos. Mag. **83**, 1533 (2003).
[24] R. A. Jackson, A. D. Murray, J. H. Harding, and C. R. Catlow, Philos. Mag. A **53**, 27 (1986).
[25] K. Kawamura, *Molecular Dynamics Simulations*, F. Yonezawa Ed., *Springer Series in Solid-State Sciences*, Vol. 103, Berlin: Springer, 88 (1992).
[26] P. M. Morse, Phys. Rev. **34**, 57 (1929).
[27] W. Smith and T. R. Forester, *DL-POLY is a Package of Molecular Simulations Subroutines*, Nr Warrington, Copyright: The Council for the Central Laboratory of the Research Councils, Daresbury Laboratory at Daresbury, (1996).
[28] S. W. De Leeuw, J. W. Perram, and E. R. Smith, Proc. R. Soc. London A **373**, 27 (1980).
[29] L. Verlet, Phys. Rev. **159**, 98 (1967).
[30] D. G. Martin, J. Nucl. Mater. **152**, 94 (1988).
[31] M. P. Allen and D. J. Tildesley, *Computer Simulation of Liquids*, Oxford: Clar-endon Press, 60 (1987).
[32] M. A. Bredig, Colloq. Int. CNRS **205**, 183 (1971).
[33] L. Eyring and M. O'Keefe, *The Chemistry of Ex-tended Defects in Non-Metallic Solids*, Elsevier Amster-dam, (1970).
[34] W. van Goal, *Fast Ions Transport in Solids*, Amsterdam: Elsevier, (1973).
[35] J. Ralph, J. Chem. Soc. Faraday Trans. 2 **83**, 1253 (1987).
[36] P. Browning, G. J. Hyland, and J. Ralph, High. Temp. High. Press. **15**, 169 (1983).
[37] R. L. June, A. T. Bell, and D. N. Theodorou, J. Phys. Chem. **94**, 8232 (1990).
[38] G. C. Allen and N. R. Holmes, Appl. Spectrosc. **48**, 525 (1994).
[39] G. L. Powell, A. Dobbins, S. S. Cristy, T. L. Cliff, H. M. Meyer III, J. Lucania, and M. Milosevic, SPIE **2089**, 214 (1994).
[40] E. Yakub, J. Chem. Phys. **127**, 094508 (2007).

DOI:10.1088/1674-0068/24/04/399-404